Extracardiac septum transversum/proepicardial endothelial cells pattern embryonic coronary arterio–venous connections

Elena Cano[a,b,c], Rita Carmona[a,d], Adrián Ruiz-Villalba[a,e], Anabel Rojas[f,g], You-Ying Chau[h,i], Kay D. Wagner[j], Nicole Wagner[j], Nicholas D. Hastie[h,i], Ramón Muñoz-Chápuli[a,d], and José M. Pérez-Pomares[a,d,1]

[a]Department of Animal Biology, Faculty of Sciences, Instituto de Investigación Biomédica de Málaga (IBIMA), University of Málaga, 29071 Málaga, Spain; [b]Group of Cardiovascular Genetics, Department of Vertebrate Genomics and Cardiovascular Genetics, Experimental and Clinical Research Center, Charité-Universitätsmedizin Berlin, Berlin 13125, Germany; [c]Max Delbrück Center for Molecular Medicine, Berlin 13125, Germany; [d]Andalusian Center for Nanomedicine and Biotechnology (BIONAND), 29590 Málaga, Spain; [e]Department of Anatomy, Embryology and Physiology, Academic Medical Center-University of Amsterdam, AZ1105 Amsterdam, The Netherlands; [f]Centro Andaluz de Biología Molecular y Medicina Regenerativa, 41092 Sevilla, Spain; [g]Centro de Investigación Biomédica en Red de Diabetes y Enfermedades Metabólicas Asociadas, 41092 Sevilla, Spain; [h]Medical Research Council Human Genetics Unit, Western General Hospital, EH4 2XU, Edinburgh, United Kingdom; [i]Institute of Genetics and Molecular Medicine at the University of Edinburgh, Western General Hospital, EH4 2XU, Edinburgh, United Kingdom; and [j]Institut de Biologie Valrose, Université Nice Sophia, CNRS, INSERM, 06108 Nice, France

Recent reports suggest that mammalian embryonic coronary endothelium (CoE) originates from the sinus venosus and ventricular endocardium. However, the contribution of extracardiac cells to CoE is thought to be minor and nonsignificant for coronary formation. Using classic ($Wt1^{Cre}$) and previously undescribed ($G2$-$Gata4^{Cre}$) transgenic mouse models for the study of coronary vascular development, we show that extracardiac septum transversum/proepicardium (ST/PE)-derived endothelial cells are required for the formation of ventricular coronary arterio–venous vascular connections. Our results indicate that at least 20% of embryonic coronary arterial and capillary endothelial cells derive from the ST/PE compartment. Moreover, we show that conditional deletion of the ST/PE lineage-specific Wilms' tumor suppressor gene ($Wt1$) in the ST/PE of $G2$-$Gata4^{Cre}$ mice and in the endothelium of $Tie2^{Cre}$ mice disrupts embryonic coronary transmural patterning, leading to embryonic death. Taken together, our results demonstrate that ST/PE-derived endothelial cells contribute significantly to and are required for proper coronary vascular morphogenesis.

coronary endothelium | septum transversum | proepicardium | Gata4 | Wt1

The coronary vascular system, whose function is necessary to sustain late embryonic and postnatal cardiac function, is formed by a complex network of blood vessels, including arteries, arterioles, capillaries, venules, and veins (1). Recent reports indicate that various sources of endothelial cells contribute to the mammalian embryonic coronary system (2–4). However, the specific fate and function of these different endothelial cell pools during coronary vascular morphogenesis is the subject of intense controversy (5).

Two endocardial populations have been reported to participate in the building of the embryonic coronary vascular system. The first derives from the sinus venosus endocardium, which sprouts to give rise to the nascent $Apelin^+$ coronary vasculature (2). A careful analysis of this study suggests that the sinus venosus endocardium, which is able to vascularize subepicardial and myocardial heart layers, mainly provides a cellular scaffold for the development of coronary veins (CoV). Accordingly, a second source of coronary endothelium (CoE) has been identified in the ventricular endocardium ($Nfatc1^+$ lineage), which contributes massively to coronary arterial (CoA) endothelium (3, 6).

A third disputed source of CoE is the proepicardium (PE), a structure that comprises epicardial progenitor cells. The PE protrudes from the septum transversum (ST), a folding of the lateral mesoderm that initiates the separation of thoracic and abdominal cavities in mammals (7). Although in vivo cell tracing and in vitro culture of avian PE cells clearly shows that PE cells can differentiate into CoE (8, 9), data from studies in mammals claimed the

contribution of PE to CoE is minor (10–12). The so-called "epicardial" Cre constructs used in these studies are based on the expression of genes such as $Gata5$, $Tbx18$, or Wilms' tumor suppressor ($Wt1$) (Table S1), all of which are expressed by both PE and ST cells, thus confirming that these two tissues form an ontogenetic and histomorphological continuum. Such continuum makes it difficult to distinguish between ST and PE cells based on their gene-expression profile. Interestingly, recent results indicate that the murine PE is constituted of different cell lineages, including a significant number of endothelial progenitors (13). Because the final fate of these cells, the extent of their contribution, and their specific role during coronary blood vessel morphogenesis remain unknown, we aimed at studying these complex aspects of coronary development.

Results

G2-$Gata4$ Enhancer-Driven Reporter Expression Labels Septum Transversum/Proepicardium Cells. At embryonic day (E)9.5, G2-$Gata4^{LacZ}$ mice display reporter activity in the septum transversum/proepicardium (ST/PE) but not in heart tissues (myocardium, endocardium) (Fig. 1A). At E11.5, G2-$Gata4^{LacZ}$ expression remains

Significance

Here we show, for the first time to our knowledge, that septum transversum/proepicardium (ST/PE)-derived endothelial cells are required for proper coronary blood vessel morphogenesis. We used different mouse transgenic lines to show that the ST/PE contributes to coronary endothelium and that the endocardium is not the only developmental origin of this tissue. Our results indicate that ST/PE-derived endothelial cells preferentially incorporate into prospective coronary arteries and capillaries but not veins. Deletion of the epicardial and coronary developmental regulator Wilms' tumor suppressor gene from both the ST/PE and embryonic endothelial cells reveals that ST/PE endothelial cells are required for the establishment of coronary arterio–venous connections through the ventricular wall and thus are necessary for the completion of coronary vascularization.

confined mainly to the mesenchyme surrounding the liver (14); weak X-gal staining also is observed in the myocardium of sinus venosus horns (Fig. 1B). Cre recombinase protein is found only in the sinus venosus myocardium and aortic walls (Fig. S1 A and C) and is not present in any other cardiac region (Fig. S1 B–D).

G2-*Gata4* Lineage Tracing Identifies the ST/PE Contribution to CoE. To trace G2-*Gata4* ST/PE cells throughout embryonic development, we crossed the G2-*Gata4*[Cre] line with *Rosa26-YFP* reporter mice. The resulting offspring (hereafter, G2[CreYFP+]) display permanent YFP expression in the ST/PE (Fig. 1 C and D), epicardium, and epicardial-derived cells (EPDCs) (Fig. 1 E and F'). E9.5 G2[CreYFP+] ST/PE tissue and some epicardial cells express GATA4 protein (Fig. 1C). WT1 (Wilms' tumor suppressor-1) protein is ubiquitous in the epicardium (Fig. 1D). Some ST/PE (Fig. 1E) and epicardial (Fig. 1 E, F, and F') WT1^{+} cells are G2[CreYFP−], suggesting that *Wt1* expression may occur in epicardial cells that do not belong to the G2-*Gata4* population. WT1 protein is reduced progressively from E11.5 through E12.5 as G2[CreYFP+] cells migrate from the subepicardium into the myocardial layers (Fig. 1F'). At these stages, *Wt1* gene expression is confined to the epicardium and early EPDCs (Fig. 1G). From E12.5 onwards, numerous ST/PE-derived G2[CreYFP+] intramyocardial cells incorporate into developing coronary blood vessels. CD31^{+} (Fig. 1 H–J) and isolectin B4^{+} (IB4) endothelial cells intermingled with G2[CreYFP-] cells in a salt-and-pepper pattern (Fig. 1 I–L and Movie S1), whereas G2[CreYFP+]/α-smooth muscle actin (α-SMA)[+] coronary smooth muscle cells (CoSM) formed continuous, large domains of the medial blood vessel wall. Many G2[CreYFP+]/IB4^{+} CoE cells accumulated NOTCH1 intracellular domain (N1ICD) in their nucleus (Fig. 1 K and L).

No G2[CreYFP+] cells are found in the sinus venosus endocardium (Fig. S1E), but some G2[CreYFP+]/CD31^{+} cells are present in the ventricular endocardium, suggesting an early contribution of ST/PE

cells to this tissue (Fig. S1F). Chimeric transplantation of quail PE (Fig. S1 G and H) or ST (Fig. S1 I–L) tissue into chick host hearts confirms that ST/PE endothelial cell incorporation in the developing coronary vessels and CoE is a normal event. To verify the vascular potential of the ST/PE, *Scl/Tal1* and *Vegfr2* expression was confirmed in ST/PE cells (Fig. S2A), and the vasculogenic potential of ST/PE was tested in vivo and in vitro (Fig. S2 B–F).

Wt1-Driven GFP Expression Is a Bona Fide Marker for Early Epicardium, EPDCs, and Coronary Blood Vessels. Because *Wt1* is also known to be a marker of ST/PE cells (15, 16), we first studied its expression pattern in *Wt1*[GFP] knockin mouse embryos. At E10.5, Wt1 protein and Wt1-driven GFP expression overlap in space and time and are restricted to the primitive epicardium (Fig. 2A), confirming that the *Wt1*[GFP] knockin mouse faithfully recapitulates native *Wt1* gene activity. At E11.5–E12.5, *Wt1* expression is detected in epicardial cells and EPDCs, which accumulate at the ventricular, atrio–ventricular, and interventricular subepicardium (Fig. 2 A–C). No CD31 expression is detected in *Wt1*[GFP+] epicardium or EPDCs before E11.5 (Fig. 2C). At E12.5, a primary coronary vascular plexus has formed in the ventricles, and GFP expression is identified in a significant proportion of subepicardial and intramyocardial CD31^{+} cells of the developing coronary vasculature (Fig. 2 D and E–E''). Some *Wt1*[GFP+] cells display the typical spindle-shaped morphology of migratory mesenchymal cells, with their major axis oriented orthogonally with respect to the epicardial surface (Fig. 2F). Between E13.5 and 14.5, a few *Wt1*[GFP+]/CD31^{+} cells can be identified in the forming intramyocardial blood vessels (Fig. 2G) with their number decreasing at perinatal stages (E18.5) (Fig. 2H).

Wt1 Lineage Cells Incorporate in Coronary Blood Vessels. To confirm further the ST/PE contribution to the developing coronary vasculature, we selected a *Wt1*[Cre] mouse line that has been used previously to study PE and coronary development (15, 16).
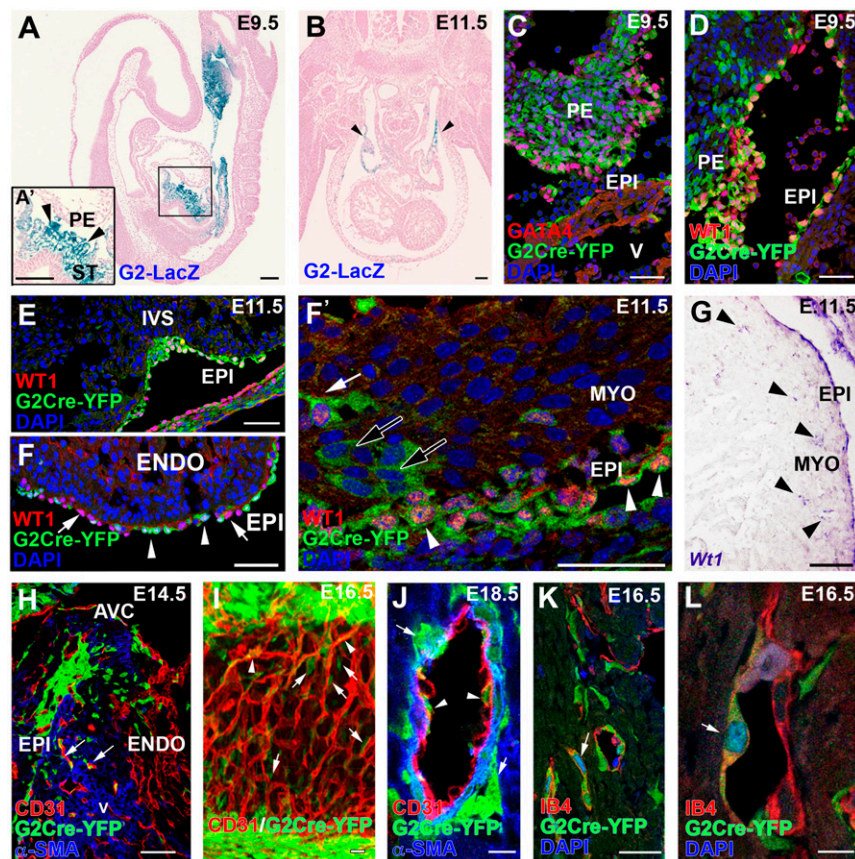
Fig. 1. ST/PE G2-*Gata4* cells throughout cardiac development. (*A* and *B*) G2-*Gata4*[LacZ] mice show reporter activity in the septum transversum (including the PE) at E9.5 (*A*) and inflow myocardium at E11.5 (*B*, arrowheads). (*C* and *D*) Immunohistochemistry of G2-*Gata4*[CreYFP+] samples illustrates the expression of GATA4 (*C*) and WT1 (*D*) proteins in G2-*Gata4*[CreYFP+] cells at E9.5 PE. (*E–F'*) G2-*Gata4*[CreYFP] mice show an increasing number of G2-*Gata4*[CreYFP+] cells from the developing epicardium in subepicardial and intramyocardial areas between stages E10.5 and E14.5. The epicardium comprises WT1^{+}/G2-*Gata4*^{+} (arrowheads) and WT1^{+}/G2-*Gata4*^{−} cells (*F*, arrows). A few EPDCs retain WT1 expression transiently (*F* and *F'*, white arrow), but other EPDCs do not (*F'*, black arrows). (*G*) *Wt1* gene expression is conspicuous in the epicardium but is restricted to a few EPDCs (arrowheads). (*H*) Progressive expansion of EPDCs through the myocardial walls at E14.5–18.5 parallels G2-*Gata4*[CreYFP+] incorporation in developing coronary blood vessels (arrows). (*I* and *J*) 3D reconstructions (*I*) and tissue section analysis (*J*) of the developing coronary vasculature allow perivascular cells (arrows in *I* and *J*) to be distinguished from G2-*Gata4*[CreYFP+] CoE cells (arrowheads in *I* and *J*). (*K* and *L*) Identification of active Notch1 signaling by Notch1 intracellular domain (N1ICD) nuclear localization confirms the arterial nature of these vessels (arrows). A, atrium; AVC, atrio–ventricular canal; ENDO, endocardium; EPI, epicardium; IVS, interventricular septum; MYO, myocardium; PE, proepicardium; ST, septum transversum; V, ventricle. (Scale bars: 100 μm in *A* and *B*; 50 μm in *C–H*; 40 μm in *I*; 10 μm in *J*; 25 μm in *K*; 5 μm in *L*.)

DEVELOPMENTAL BIOLOGY
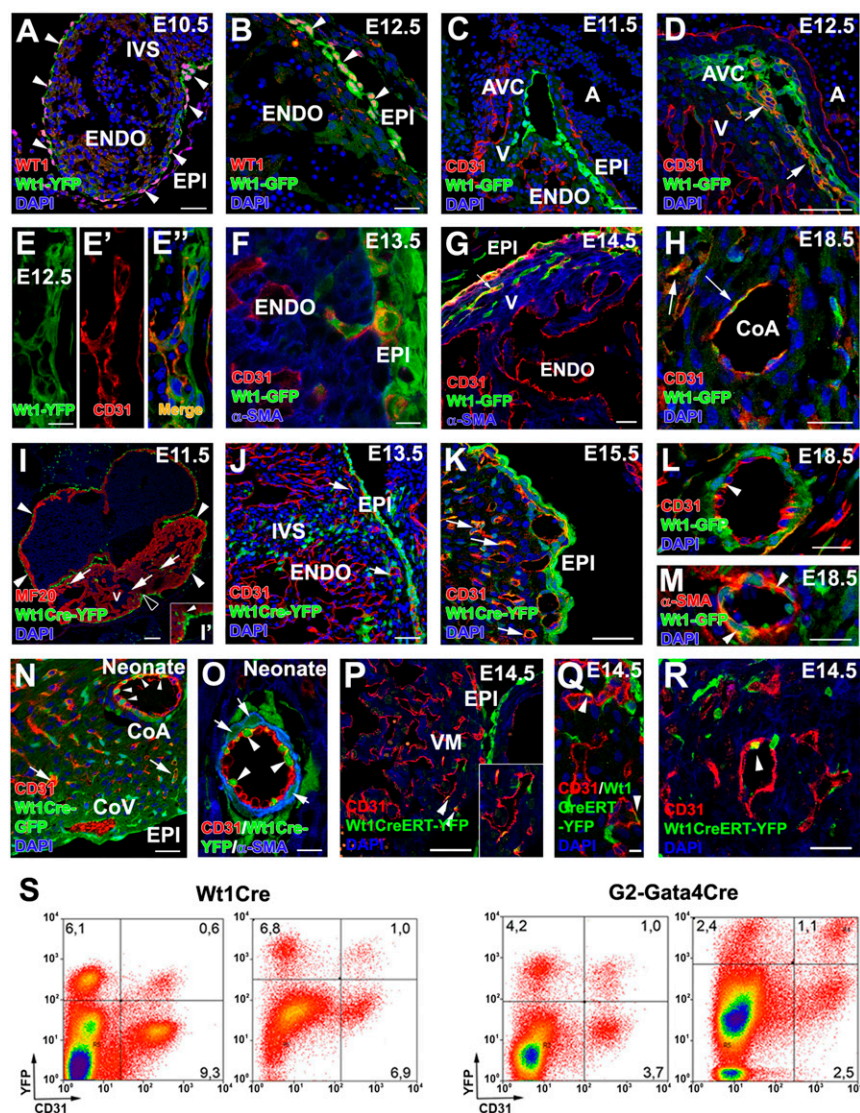
Fig. 2. *Wt1*-expressing cells and their progeny contribute to CoE. (*A* and *B*) WT1 protein is ubiquitously expressed in epicardial cells and EPDCs at E10.5–E12.5, extensively overlapping with *Wt1* promoter-driven *GFP* expression (arrowheads). (*C–G*) Reporter expression in *Wt1*^{GFP} embryos can be observed in the CD31$^+$ subepicardial (*E–E"*) and intramyocardial (*F* and *G*) coronary vasculature at E12.5–E14.5 (arrows in *D* and *G*), but not at earlier developmental stages (*C*). (*H*) A few *Wt1*$^{GFP+}$/CD31$^+$ cells are still found at perinatal stages (arrows). (*I*, *I'*, and *J*) Early *Wt1*$^{CreYFP+}$ cells form the epicardium (arrowheads in *I*; the area marked with a black arrowhead is magnified in *I'*) and the first EPDCs (arrows in *J*). At E11.5 many *Wt1*$^{CreYFP+}$ epicardial cells show morphological EMT features (arrowhead in *I'*). (*J* and *K*) The lineage reporter colocalizes with the vascular marker CD31 in the subepicardial and intramyocardial coronary plexus between E13.5 (*J*) and E15.5 (*K*) (arrows). (*L–O*) Perinatal (*L* and *M*) and neonatal (*N* and *O*) hearts show *Wt1*$^{CreYFP+}$ cells incorporated in the CoE (arrowheads in *L* and *O*) and CoSM layers of large CoA (arrowheads in *M* and arrows in *O*) as well as in capillaries (arrow in *N*). (*P–R*) *Wt1*^{CreERT2};*Rosa26*-YFP embryos induced with tamoxifen at E9.5 show YFP$^+$ cell incorporation in coronary vessels at E.14.5 (arrowheads). (*S*) Representative cytograms of dissociated ventricles from midgestation embryos and neonates. Numbers indicate percentages of total events. Both the *Wt1*$^{CreYFP+}$ and G2$^{CreYFP+}$ populations include CD31$^+$ in cells. A, atrium; AVC, atrio–ventricular canal; CoA, coronary artery; CoV, coronary vein; ENDO, endocardium; EPI, epicardium; IVS, interventricular septum; V, ventricle. (Scale bars: 100 μm in *I*; 50 μm in *A*, *C*, *D*, *J*, *M*, *N*, and *P*; 25 μm in *B*, *F–H*, *K*, and *L*; 25 μm in *R*; 10 μm in *E–E"* and *O*; 5 μm in *Q*.)

Crossing these mice with the *Rosa26-YFP* reporter line allows the tracing of the *Wt1* cell lineage (hereafter, *Wt1*$^{CreYFP+}$). At E9.0–9.5, no *Wt1*$^{CreYFP+}$ cells are seen in heart, except for a few isolated cardiomyocytes (*Wt1*$^{CreYFP+}$/α-SMA$^+$) that form part of the cardiac chamber walls (Fig. S3*A*). None of these cells express the vascular marker CD31 (Fig. S3*B*). Between E10.5 and E11.5 almost all epicardial cells and the majority of subepicardial EPDCs are *Wt1*$^{CreYFP+}$ (Fig. 2*I*). A fraction of *Wt1*$^{CreYFP+}$ epicardial cells apparently were detaching from the epicardial lining (Fig. 2*F*). Active epicardial epithelial-to-mesenchymal transition (EMT) was confirmed by time-lapse analysis of *Wt1*$^{CreYFP+}$ whole-heart explants (Movie S2). At these stages, a minor number of *Wt1*$^{CreYFP+}$/CD31$^+$ cells could be identified in the endocardial layer (Fig. S3*C*). From E12.5 onwards, subepicardial and intramyocardial *Wt1*$^{CreYFP+}$ cells increase (Fig. 2 *J* and *K*). *Wt1*$^{CreYFP+}$ cells are CD31$^+$ endothelial (Fig. 2*L*) and αSMA$^+$ smooth muscle (Fig. 2*M*) cells of the intramyocardial coronary vessels (prospective CoA). Neonatal arterial CoE was found to be a mosaic of *Wt1*$^{CreYFP+}$ and *Wt1*$^{CreYFP-}$ cells. Perivascular cells closer to the CoE expressed α-SMA, but only a fraction of them was *Wt1*$^{CreYFP-}$ (Fig. 2 *N* and *O*). To confirm that Wt1$^+$ ST/PE cells contribute to the formation of coronary vessels, *Wt1*^{CreERT2} mice were crossed with the *Rosa26-YFP* line, and recombination was induced with tamoxifen at PE stages (E9.0). At E14.5 all embryos showed a reduced but evident contribution to the developing CoE (Fig. 2 *P–R*).

Wt1 and G2-*Gata4* ST/PE Cell Populations Contribute Differentially to the CoE. To quantify further the contribution of PE cells to the embryonic CoE, we analyzed G2^{CreYFP} and *Wt1*^{CreYFP} dissociated ventricles by FACS. CD31 was used as pan-endothelial marker. From midgestation to birth, *Wt1*$^{CreYFP+}$ cells account for 6.5 of total ventricular cells at E12.5 and 8% in neonates. At E12.5, the percentage of G2$^{CreYFP+}$ cells is 9.1%; this percentage decreases to 4% of total ventricular cells by the end of gestation (Fig. S3*D*). Interestingly, the cytometric analysis reveals that the percentage of CD31$^+$/G2$^{CreYFP+}$ cells is higher than that of CD31$^+$/*Wt1*$^{CreYFP+}$ cells: By E17.5, 22.7 ± 4.2% of all CD31$^+$ cells are G2$^{CreYFP+}$ (*n* = 4), and this percentage reaches 35.7 ± 5.0% in neonates (*n* = 3). Only 11.3 ± 1.9% of CD31$^+$ cardiac cells are *Wt1*$^{CreYFP+}$ by E18.5 (*n* = 6) (Fig. 2*S*). This differential contribution of the two lineages to the CoE was confirmed by quantitative image analysis in E18.5 G2^{CreYFP} and *Wt1*^{CreYFP} embryos. When only the compact ventricular layer (i.e., excluding the endocardium, epicardium, and trabeculae) is considered, 49.3 ± 13.9% of CD31$^+$ cells are G2$^{CreYFP+}$, and only 25.1 ± 4.1% are Wt1$^{CreYFP+}$. The percentages of ST/PE-derived endothelial cells obtained after the image analysis are higher than those from the cytometry analysis because of the exclusion of the endocardial

cells, but the 1:2 proportion between Wt1$^{CreYFP+}$ and G2$^{CreYFP+}$ cells remains evident. Thus, the more stringent estimate of these data indicates that at least 20% of embryonic CoE are ST/PE derivatives.

Wt1 Expression in G2-Gata4 Cells Is Required for CoA Development. G2-Gata4^{Cre}–driven Wt1 deletion (G2^{Cre};Wt1$^{LoxP/LoxP}$) severely impairs the development of coronary vasculature, causing embryonic lethality around E15.5 (Fig. 3 A–F). 3D reconstruction of CoE (CD31$^+$) shows that mutant embryos develop tortuous and sinusoidal irregular vessels that fail to progress transmurally and do not complete ventricular myocardium invasion (Fig. 3 A–D and Movies S3 and S4). Normal CoA are missing in the mutants, which also display a thin ventricular compact myocardium (Fig. 3 B and E). Effective Wt1 deletion in these embryos was confirmed by the absence of WT1 protein and the marked decrease of RALDH2, a known Wt1 target (17) (Fig. S4). However, the epicardium remains intact in the mutants (Fig. 3F). Prompted by the recorded N1ICD nuclear accumulation in G2$^{CreYFP+}$ CoE, we tested whether this endothelial compartment is affected after G2-mediated Wt1 deletion (G2-Gata4^{Cre};Wt1$^{LoxP/LoxP}$). N1ICD$^+$ cells are frequent in capillaries and putative CoA endothelium; however, mutant N1ICD$^+$ CoE does not form normal transmural coronary blood vessels, failing to connect to the deeper vascular elements of the developing coronary vasculature (Fig. 3 C–F).

Wt1 Systemic Deletion Results in a Severe Coronary Phenotype. Because the E10.5 epicardial Wt1-expressing population encompasses all epicardial G2-Gata4 cells, we decided to cross tamoxifen-inducible CAGG^{CreERT2} and Wt1$^{LoxP/GFP}$ mouse lines to generate systemic Wt1 mutants at early epicardial stages. CAGG-Cre–mediated Wt1 deletion at E10.5 results in embryonic death by E13.5. These embryos display a sharp impairment of EPDC migration into the compact ventricular myocardium and disruption of intramyocardial coronary vessel morphogenesis, as

revealed by the GFP copy carried by mutant mice (Fig. 3 G–I''). However, the subepicardial coronary vasculature is still formed. This phenotype is more severe than that of G2^{Cre};Wt1$^{LoxP/LoxP}$ mutants (compare Fig. 3 A–F and Fig. 3 G–I'').

Conditional Wt1 Endothelial Deletion Reproduces G2-Gata4^{Cre};Wt1$^{LoxP/LoxP}$ Coronary Defects. To prove that coronary vascular defects in G2-Gata4^{Cre};Wt1$^{LoxP/LoxP}$ mutants are not caused by disrupted epicardial signaling, we crossed Tie2^{CreERT2} (18) and Wt1$^{LoxP/LoxP}$ mice to create endothelial cell-specific Wt1 knockouts (19). Tamoxifen was injected at E10; the specificity of tamoxifen-induced recombination is shown in Fig. S5. Heart morphology is similar in wild-type and mutant animals (E16.5), which do not show compact myocardial thinning (Fig. 4 A and B). WT1 protein is found in some coronary vascular structures and isolated EPDCs of wild-type animals but is much reduced in Tie2^{CreERT2};Wt1$^{LoxP/LoxP}$ mutants (Fig. 4 C–E). Wt1 gene expression also is down-regulated significantly in mutant embryos (Fig. 4F). CD31 immunostaining of wild-type and mutant samples reveals a marked reduction in the number of coronary vessels, especially transmural vessels connecting endocardial and epicardial elements of the coronary vasculature (Fig. 4 G and H). Reduced coronary vascularization in mutant hearts was confirmed by the analysis of the area occupied by CD31$^+$ cells (Fig. 4I) and by down-regulation of the CD31 gene (Fig. 4J).

Discussion

To understand the morphogenesis of the coronary vascular system fully, we need to uncover the molecular and cellular mechanisms that integrate different endothelial compartments (i.e., the embryonic arterial and venous coronary vasculature) into a single, continuous vascular bed and to identify the origin of coronary endothelial progenitors (1). In this regard, Katz and collaborators (13) have proven that the PE comprises several cell compartments (identified by either Scleraxis or Semaphorin3D gene expression) that contribute differentially to CoE. However, the
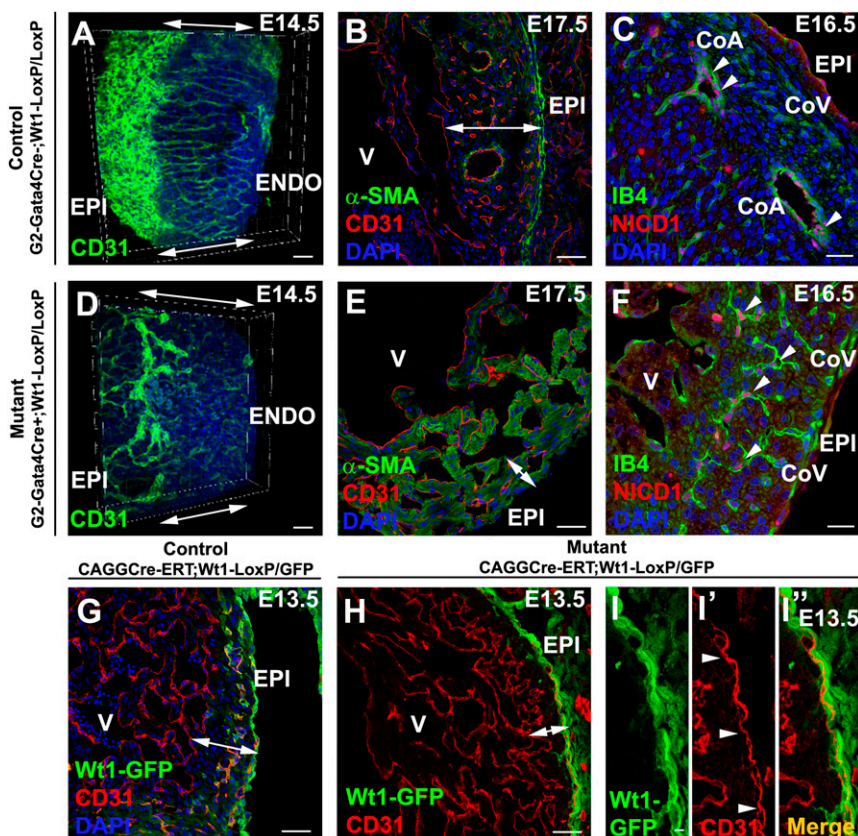
Fig. 3. G2-Gata4 and conditional systemic Wt1 deletion disrupt CoA formation. (A–F) G2-Gata4^{Cre}; Wt1$^{LoxP/LoxP}$ embryonic CoE structures are dysmorphic and fail to contact the endocardium (compare double-headed arrows in A and D and compare Movie S3 with Movie S4). The mutants show dramatic reduction of compact ventricular myocardium thickness (compare double-headed arrows in B and E). N1ICD immunohistochemistry identifies dysmorphic intramyocardial vessels as developing CoA (arrowheads in C and F), whereas subepicardial vascular structures are N1ICD$^-$ (prospective CoV). (G and H) Tamoxifen-induced (E10.5) systemic Wt1 deletion sharply reduces the number of developing intramyocardial blood vessels. (I–I'') Subepicardial blood vessels (arrowheads) form normally. CoA, coronary artery; CoV, coronary vein; ENDO, endocardium; EPI, epicardium; V, ventricle. (Scale bars: 50 μm in A and B; 25 μm in C; 50 μm in D, E, G–I; 25 μm in F.)
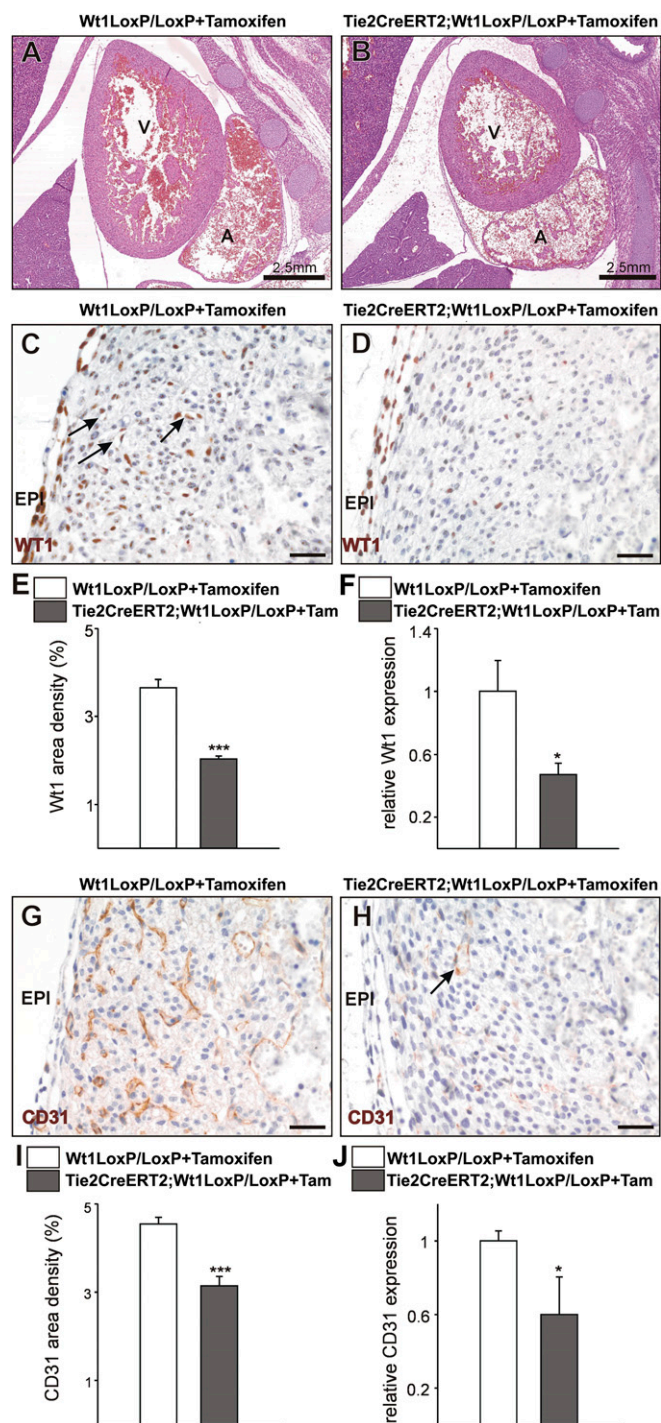
Fig. 4. Endothelial *Wt1* expression is required for coronary vessel formation. (*A* and *B*) H&E-stained sections from control *Wt1*^{LoxP/LoxP}+Tamoxifen (*A*) and mutant *Tie*^{CreERT2};*Wt1*^{LoxP/LoxP}+Tamoxifen (*B*) E16.5 embryos. (*C–F*) The WT1⁺ cell contribution to coronary vessels (arrows in *C*) is reduced in the mutants (*D* and *E*), and *Wt1* gene expression in E16.5 mutant hearts is reduced (*F*). (*G* and *H*) E16.5 mutant embryonic hearts show a decrease in compact ventricular wall coronary CD31⁺ cells (arrow in *H*; compare with *G*). (*I* and *J*) Quantification of the area occupied by CD31⁺ cells (*I*) and *CD31* gene expression (*J*) in E16.5 hearts. A, atrium; EPI, epicardium; V, ventricle. (Scale bars: 50 μm.) Data are mean ± SEM; *P < 0.05, ***P < 0.001.

specific developmental function of ST/PE-derived CoE during coronary morphogenesis has remained unknown.

Our results indicate that the G2-*Gata4* enhancer, to our knowledge used here for the first time to study coronary vascular development, is as a bona fide marker of ST/PE cells, being active only at the extracardiac ST/PE location (E9.5) and not in heart tissues proper. G2-*Gata4*-driven reporter expression first is confined to the epicardium and its mesenchymal derivatives (1, 20–22) and then expands to the CoE.

Wt1^{CreYFP+} ST/PE cells also contribute to the CoE, although they are less abundant than G2-*Gata4*^{CreYFP+} cells, suggesting an early specification of this endothelial lineage. This finding also explains why other studies, relying mostly on genetic tracking of the *Wt1* cell lineage, deemed ST/PE contribution to the CoE to be negligible, especially when inducible mouse Cre lines are used (e.g., ERT2). The extent of the induced recombination depends on the stage of development considered, the dose and procedure for delivering tamoxifen, and the genetic construct itself. It is possible that the differences in the relative abundance of *Wt1*^{CreYFP+} and G2-*Gata4*^{CreYFP+} cells in the developing heart could relate to the reported de novo expression of WT1 protein in cardiac vessels following myocardial infarction (23, 24). Whether this *Wt1* activation is linked to the developmental origin of these cells (25) or instead represents an ectopic activation of the gene in response to hypoxia (26) has been discussed extensively (27). However, the lack of activation of the G2 enhancer within heart tissues strongly suggests an ST/PE, extracardiac origin for G2-*Gata4*^{CreYFP+} cells, whose endothelial differentiation potential is higher than that shown by Wt1^{CreYFP+} cells. Our most restrictive estimate of G2-*Gata4*^{CreYFP+} and Wt1^{CreYFP+} cell incorporation in the CoE (a minimum of 20%) is compatible with the reported variable endocardial contribution to coronary vasculature, ranging roughly from 70–40% of embryonic CoE cells (3).

Our cell-tracing analysis shows a preferential incorporation of ST/PE endothelial cells to intramyocardial coronary blood vessels (prospective CoA, arterioles, and capillaries) and suggests a different developmental origin for CoA and CoV. This concept is supported further by the CoA (but not CoV) endothelial phenotype found in mouse embryos with deficient epicardial NOTCH1 signaling (15) and the anomalies found in the prospective intramyocardial CoA endothelium (N1ICD⁺) of the *Wt1* mutants we have described in this study. Such anomalies involve the disruption of the transmural connection between prospective intramyocardial arteries and prospective subepicardial veins. Coronary anomalies recorded in *Tie2*^{CreERT2};*Wt1*^{LoxP/LoxP} mutants, which display a reduction in both WT1⁺ and CD31⁺ cells in the ventricular myocardial walls and an anomalous organization of embryonic coronary vessels, confirm that the G2-*Gata4*–mediated loss of Wt1 in ST/PE cells primarily affects the CoE.

In summary, our work unambiguously shows that the ST/PE significantly contributes cells to the CoE that are necessary for proper coronary vascular morphogenesis (Fig. 5) and suggest that the ST/PE-derived component of CoE is mechanistically related to CoA rather than to CoV, revealing a functional role for these cells in transmural arterio–venous patterning of the coronary vascular tree, most likely via the segregation of NOTCH⁺ and NOTCH⁻ endothelial domains. This study also supports the idea that CoE is a developmental mosaic formed from different sources of endothelial cells and opens new perspectives on the understanding of congenital coronary anomalies and adult coronary endothelium malfunction.

Methods

Additional methods are described in *SI Methods*.

Mouse Lines and Embryo Extraction. The procedures for animal experiments were approved by the Committee on the Ethics of Animal Experiments of the University of Malaga (procedure code 2009-0037), and also followed the guidelines of the French Coordination Committee on Cancer Research and local Home Office regulations. The animals used in our research program were handled in compliance with the institutional and European Union guidelines for animal care and welfare.

All embryos were staged from the time point of vaginal plug, which was designated as E0.5. Embryos were excised and washed in PBS before further processing.
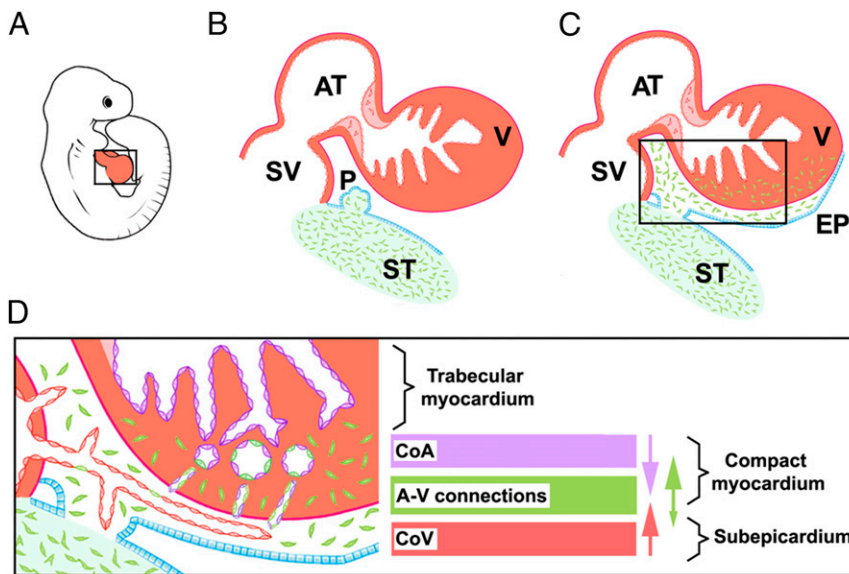
Fig. 5. A model of the EPDC contribution to the CoE. ST/PE-derived endothelial cells (green) give rise to the epicardium and EPDCs (*A–C*) and are incorporated in intramyocardial CoA and capillary endothelium (*D*). Major transmural endothelial cell flows are indicated by arrow color; the arrow size estimates the frequency of the events. A, atrium; A-V, arterio–venous; CoA, coronary arteries; CoV: coronary veins; EPI: epicardium; PE: proepicardium; ST, septum transversum; SV, sinus venosus; V, ventricle.

Tissue Sampling for Fluorescent Reporter and Immunohistochemical Analysis. Embryos were fixed in 2–4% fresh paraformaldehyde solution in PBS for 2–8 h, washed in PBS, cryoprotected in sucrose solutions, embedded in optimum cutting temperature (OCT) embedding compound (Tissue-Tek), and frozen in liquid N_2-cooled isopentane. Immunofluorescence staining was performed as described elsewhere (see *SI Methods* for a detailed protocol). All images were captured on a Leica SP5 confocal microscope.

Quantitative and Semiquantitative RT-PCR of Mouse Tissue. Total RNA was isolated from embryonic hearts using the TRIzol reagent (Invitrogen). First-strand cDNA synthesis was performed with 0.5 μg of total RNA using oligo(dT) and random primers and superscript III reverse transcriptase (Invitrogen).

1. Pérez-Pomares JM, de la Pompa JL (2011) Signaling during epicardium and coronary vessel development. *Circ Res* 109(12):1429–1442.
2. Red-Horse K, Ueno H, Weissman IL, Krasnow MA (2010) Coronary arteries form by developmental reprogramming of venous cells. *Nature* 464(7288):549–553.
3. Wu B, et al. (2012) Endocardial cells form the coronary arteries by angiogenesis through myocardial-endocardial VEGF signaling. *Cell* 151(5):1083–1096.
4. Tian X, et al. (2014) Vessel formation. De novo formation of a distinct coronary vascular population in neonatal heart. *Science* 345(6192):90–94.
5. Tian X, Pu WT, Zhou B (2015) Cellular origin and developmental program of coronary angiogenesis. *Circ Res* 116(3):515–530.
6. Zhang Z, Zhou B (2013) Accelerated coronary angiogenesis by vegfr1-knockout endocardial cells. *PLoS One* 8(7):e70570.
7. Männer J, Pérez-Pomares JM, Macías D, Muñoz-Chápuli R (2001) The origin, formation and developmental significance of the epicardium: A review. *Cells Tissues Organs* 169(2):89–103.
8. Guadix JA, Carmona R, Muñoz-Chápuli R, Pérez-Pomares JM (2006) In vivo and in vitro analysis of the vasculogenic potential of avian proepicardial and epicardial cells. *Dev Dyn* 235(4):1014–1026.
9. Mikawa T, Fischman DA (1992) Retroviral analysis of cardiac morphogenesis: Discontinuous formation of coronary vessels. *Proc Natl Acad Sci USA* 89(20):9504–9508.
10. Merki E, et al. (2005) Epicardial retinoid X receptor alpha is required for myocardial growth and coronary artery formation. *Proc Natl Acad Sci USA* 102(51):18455–18460.
11. Cai CL, et al. (2008) A myocardial lineage derives from Tbx18 epicardial cells. *Nature* 454(7200):104–108.
12. Zhou B, et al. (2008) Epicardial progenitors contribute to the cardiomyocyte lineage in the developing heart. *Nature* 454(7200):109–113.
13. Katz TC, et al. (2012) Distinct compartments of the proepicardial organ give rise to coronary vascular endothelial cells. *Dev Cell* 22(3):639–650.
14. Rojas A, et al. (2005) Gata4 expression in lateral mesoderm is downstream of BMP4 and is activated directly by Forkhead and GATA transcription factors through a distal enhancer element. *Development* 132(15):3405–3417.
15. del Monte G, et al. (2011) Differential Notch signaling in the epicardium is required for cardiac inflow development and coronary vessel morphogenesis. *Circ Res* 108(7):824–836.
16. Wessels A, et al. (2012) Epicardially derived fibroblasts preferentially contribute to the parietal leaflets of the atrioventricular valves in the murine heart. *Dev Biol* 366(2):111–124.
17. Guadix JA, et al. (2011) Wt1 controls retinoic acid signalling in embryonic epicardium through transcriptional activation of Raldh2. *Development* 138(6):1093–1097.
18. Forde A, Constien R, Gröne HJ, Hämmerling G, Arnold B (2002) Temporal Cre-mediated recombination exclusively in endothelial cells using Tie2 regulatory elements. *Genesis* 33(4):191–197.
19. Wagner K-D, et al. (2014) The Wilms' tumour suppressor Wt1 is a major regulator of tumour angiogenesis and progression. *Nat Commun* 5:5852.
20. Gittenberger-de Groot AC, Vrancken Peeters MP, Mentink MM, Gourdie RG, Poelmann RE (1998) Epicardium-derived cells contribute a novel population to the myocardial wall and the atrioventricular cushions. *Circ Res* 82(10):1043–1052.
21. Pérez-Pomares JM, Macías D, García-Garrido L, Muñoz-Chápuli R (1998) The origin of the subepicardial mesenchyme in the avian embryo: An immunohistochemical and quail-chick chimera study. *Dev Biol* 200(1):57–68.
22. Männer J (1999) Does the subepicardial mesenchyme contribute myocardioblasts to the myocardium of the chick embryo heart? A quail-chick chimera study tracing the fate of the epicardial primordium. *Anat Rec* 255(2):212–226.
23. Wagner KD, et al. (2002) The Wilms' tumor suppressor Wt1 is expressed in the coronary vasculature. *FASEB J* 16(9):1117–1119.
24. Duim SN, Kurakula K, Goumans M-J, Kruithof BPT (2015) Cardiac endothelial cells express Wilms' tumor-1: Wt1 expression in the developing, adult and infarcted heart. *J Mol Cell Cardiol* 81:127–135.
25. Wagner N, et al. (2005) Coronary vessel development requires activation of the TrkB neurotrophin receptor by the Wilms' tumor transcription factor Wt1. *Genes Dev* 19(21):2631–2642.
26. Wagner KD, et al. (2003) Oxygen-regulated expression of the Wilms' tumor suppressor Wt1 involves hypoxia-inducible factor-1 (HIF-1). *FASEB J* 17(10):1364–1366.
27. Rudat C, Kispert A (2012) Wt1 and epicardial fate mapping. *Circ Res* 111(2):165–169.
28. Hosen N, et al. (2007) The Wilms' tumor gene WT1-GFP knock-in mouse reveals the dynamic regulation of WT1 expression in normal and leukemic hematopoiesis. *Leukemia* 21(8):1783–1791.
29. Martínez-Estrada OM, et al. (2010) Wt1 is required for cardiovascular progenitor cell formation through transcriptional control of Snail and E-cadherin. *Nat Genet* 42(1):89–93.

DEVELOPMENTAL BIOLOGY